

# A trium test on beyond $\Lambda$ CDM triggering parameters.

Z. Sakr<sup>a,b,c</sup>

<sup>a</sup>Institut für Theoretische Physik, Philosophenweg 16, 69120 Heidelberg, Germany

<sup>b</sup>IRAP, Université de Toulouse, CNRS, CNES, UPS, Toulouse, France

<sup>c</sup>Faculty of Sciences, Université St Joseph; Beirut, Lebanon

E-mail: [ziad.sakr@net.usj.edu.lb](mailto:ziad.sakr@net.usj.edu.lb)

**Abstract.** We performed a Bayesian study on three beyond LCDM phenomenological triggering parameters, the growth index  $\gamma$ , the dark energy equation of state parameter  $w$  and the lensing deviation from the GR prediction parameter  $\Sigma$ , using the latest cosmological geometric, growth and lensing probes, all in a consistent implementation within the modified gravity cosmological solver code MGCLASS. We find, when we combined all our probes, i.e. the cosmic microwave background (CMB), the baryonic acoustic oscillation (BAO), the growth measurements  $f\sigma_8$  and the  $3\times 2$  points galaxy clustering and lensing cross-correlations, assuming flat space, constraints compatible with general relativity and  $\Lambda$ CDM for  $\omega = -1.025 \pm 0.045$ , and  $\Sigma = 0.992 \pm 0.022$  at the 68% level, while  $\gamma = 0.633 \pm 0.044$  is still within  $\sim 2\sigma$  from the  $\Lambda$ CDM value of  $\gamma \sim 0.55$ , and that when  $\Sigma$  is considered as constant; while  $\gamma_\ell = -0.025 \pm 0.045$  when the lensing parameter is parameterised as function of a lensing index, introduced for the first time in this work, as  $\Sigma(z) = \Omega_m(z)^{\gamma_\ell}$ .

---

## Contents

<b>1</b>	<b>Introduction</b>	<b>1</b>
<b>2</b>	<b>Theoretical context and model implementation</b>	<b>2</b>
<b>3</b>	<b>Datasets used and pipeline</b>	<b>3</b>
<b>4</b>	<b>Results</b>	<b>3</b>
<b>5</b>	<b>Conclusion</b>	<b>6</b>

---

## 1 Introduction

The cosmological standard model, dubbed  $\Lambda$ CDM, is the minimal model in concordance with current observations. The latter however still allows, though within small margins, some extensions to it, such as a different evolution for the dark energy component, or a modification of the general relativity to, either mimic the effect of dark energy (DE) or to test whether new theories could better fit the data along with the presence of a dynamical DE. We are not going to review here the many attempts to explain the origin of a constant or dynamical dark energy (see [1] and references therein) or the different modified gravity theories that could or not account for the evolution of the universe in general or its late acceleration in particular (see [2] for a review), but we just note that the landscape of possible still viable theories, albeit the fact that they have not been enough tested, has become so extended that it is becoming more difficult to test them exhaustively in a short time with every data release. This is true especially that each model would need substantial work to, first pass the theoretical conditions and not violate some fundamental physical principles, then determine the outcome of the different probes and observables within the new framework, to finally confront them to data throughout time consuming Monte Carlo Markov Chain (MCMC) Bayesian tests, the most common method commonly used to infer constraints on a specific model's parameters. Therefore many suggested to group or try to encapsulate the different extensions and modifications under parameterized models tailored to test their phenomenological imprints on the cosmological observables. A first simple way was the introduction of the parametrisation of the equation of state of dark energy  $w$  to describe DE dynamical evolution and its impact on the cosmological background as well as its induced effects on the growth of structure [3, 4]. While on the pure perturbation level, two functions  $\mu$  and  $\eta$  that alter the relations between the Newtonian and Weyl potential and the matter density contrast were also proposed [5–10], and alternatively, Effective Field Theory approach (EFT) was also introduced [11] to define a general action for a broad class of modified gravity theories with effects on the background and the perturbation sector (see [12] and references therein). Finally, more phenomenological inspired parametrizations were considered, such as one for the growth of structure found to be accurately determined by a functional form of the matter density and a growth index  $\gamma$  [13], or another one,  $\Sigma$  introduced by [9], which could parameterises the effects of a modified gravity on photon lensing. Here we are interested in constraining three of the aforementioned parameters, i.e.  $\omega$ ,  $\gamma$  and  $\Sigma$  with a combination of the latest current data. Several have tried to put constrain on one, two or a combination of the three [14, 15] without however varying

them all together maybe to limit the theoretical biases induced when their phenomenological origin are not treated in a consistent framework. Here we try to remedy for that by coherently implementing the effect from the three parameters we varied together,  $\Omega$ ,  $\gamma$  and  $\Sigma$  in the cosmological solver `MGCLASS II` [16] which is a modification to the Boltzmann solver `CLASS` [17] to account for the impact of different extensions and modified GR models on the cosmological observables in the quasi-static limit [18] or beyond [19]. This will serve to put, for the first time and within the latest current available data, constraints on these parameters when they are all varied at once, so that to verify whether their allowed values are still compatible with  $\Lambda$ CDM, but also to prepare the road for exploiting forthcoming data from the next generation stage IV surveys. Often a cosmic evolution for our or other parameterised extensions to  $\Lambda$ CDM is considered. Here we are also going to compare two chosen ones for  $\Sigma$ , a constant value and a dynamical one, with the latter inspired from the same way we parameterise the growth with  $\gamma$  but using an index we call  $\gamma_\ell$  leaving it as constant but free to vary, with the aim, among others, to investigate what would be the effect induced from considering a similar parameterization for both growth and lensing parameters.

The paper is structured as follows: in [section 2](#) we review the main equations used in the phenomenological approach to test extensions to  $\Lambda$ CDM model. In [section 3](#) we present the datasets and pipeline used for parameter estimation of the considered models. In [section 4](#), we show and discuss the results before drawing our conclusions in [section 5](#)

## 2 Theoretical context and model implementation

The evolution of perturbations in modified gravity (MG) could be described by the following relations between the time and scale potentials and the two modified gravity parameterisation  $\mu(a, k)$  and  $\Sigma(a, k)$  :

$$-k^2 \Psi(a, \vec{k}) = \frac{4\pi G}{c^2} a^2 \bar{\rho}(a) \Delta(a, \vec{k}) \times \mu(a, k), \quad (2.1)$$

$$-k^2 [\Phi(a, \vec{k}) + \Psi(a, \vec{k})] = \frac{8\pi G}{c^2} a^2 \bar{\rho}(a) \Delta(a, \vec{k}) \times \Sigma(a, k), \quad (2.2)$$

where  $\bar{\rho}\Delta = \bar{\rho}\delta + 3(aH/k)(\bar{\rho} + \bar{p})v$  with  $\Delta$  the comoving density perturbation of  $\delta = (\rho - \bar{\rho})/\bar{\rho}$ , and  $\bar{\rho}$ ,  $\bar{p}$  and  $\bar{v}$  are, respectively, the density, pressure and velocity, with the bar denoting mean quantities.  $\Phi$  and  $\Psi$  are the Bardeen potentials entering the perturbed FLRW metric in flat space, which in the Newtonian gauge is

$$ds^2 = a^2 [-(1 + 2\Psi)d\tau^2 + (1 - 2\Phi)d\vec{x}^2] . \quad (2.3)$$

The two functions  $\mu(a, k)$ , and  $\Sigma(a, k)$  encode possible deviations from GR, which is recovered when they are constant and equal to unity. The implementation of the growth index  $\gamma$  here follows the method described in [10], where however a  $\Lambda$ CDM background is assumed equivalent to a dark energy equation of state parameter  $\omega = -1$ . Here we further allow a  $\omega \neq -1$ . This will modify the dark energy density  $\rho_\Lambda$  entering  $\Omega_\Lambda$  in the Friedmann-Lemaître equations to

$$\rho_{\Lambda(mod)} = \rho_\Lambda (1 + z)^{3(1+\omega_0)}, \quad (2.4)$$

and propagate in Equ. 2.6 governing the growth of structure through  $H(a)$  and  $E_m(a)$ . Then using the system of equations above for modified gravity and the definition of the  $\gamma$  parame-

terization for the growth,

$$\Omega_m(a)^\gamma = \frac{d \log D_+}{d \log a}, \quad (2.5)$$

where  $D_+ \equiv \Delta(a)_m/a$  is the growth rate, defined in terms of the matter density perturbation  $\delta_m$ , and  $\gamma$  considered constant here (see [20, 21] for more general parameterisations) one can solve the second order equation for scale independent growth

$$\Delta''(a) + \left[ 2 + \frac{H'(a)}{H(a)} \right] \Delta'(a) - \frac{3}{2} \frac{E_m(a)}{E(a)} \mu(a) \Delta(a) = 0, \quad (2.6)$$

where prime denotes derivative with respect to  $\ln a$ ,  $E_m(a) = \Omega_m/a^3$ ,  $E(a) = H^2(a)/H_0^2$  and  $\Delta(a)$  the comoving density contrast, after combining with Equ. 2.5 and 2.4 to relate  $\gamma$ ,  $w$  and  $\mu(a)$  as:

$$\mu(a) = \frac{2}{3} \Omega_m^{\gamma-1}(a) \left[ \Omega_m^\gamma(a) + 2 - 3\gamma + 3\left(\gamma - \frac{1}{2}\right) (\Omega_m(a) + (1+w)\Omega_{DE}) \right] \quad (2.7)$$

We then end up with two independent parameters  $\gamma$  and  $w$  along with  $\Sigma(z)$  which we choose next to be, either constant, or following a parametrization function of the matter density at a given redshift to the power  $\gamma_\ell$ ,

$$\Sigma(z) = \Omega_m(z)^{\gamma_\ell}, \quad (2.8)$$

inspired from that used for the common growth index we relabel later in the dynamical  $\Sigma$  case as  $\gamma_f$  to distinguish it from our lensing index.

### 3 Datasets used and pipeline

We use CMB temperature, polarization, their cross correlations  $C_\ell$  and lensing spectrum  $D_\ell$  likelihood [22] and data released by the Planck satellite mission [23] (hereafter Plk18). We also include background observations from BAO measurements [24–26] and combine with redshift space distortion data (RSD) based on the data set compiled by [27]. We note that the latter are distinct and not correlated with the BAO data we have chosen. We end by combining with galaxy lensing, clustering and their cross correlated spectrum from the dark energy survey (DES) collaboration [28, 29] in which we limit to the linear scales. We run our MCMC using MGCLASS II [16]<sup>1</sup> which is interfaced with the cosmological data analysis code MontePython [30] in which the RSD code was first included by [31] while the DES likelihood was implemented by us based on the official public one.

### 4 Results

In Fig. 1 and 2 we show constraints on  $\Omega_m$ ,  $h$ ,  $\omega$ ,  $\gamma$ ,  $\sigma$  and  $S_8 = (\Omega_m/0.3)^{0.5} \sigma_8$ , obtained after varying all the cosmological and nuisance parameters of the probes mentioned in section 2 and that for two cases: one with a constant  $\Sigma$  and the other with our new parameterization  $\Sigma(z) = \Omega_m(z)^{\gamma_\ell}$ . For each case we start by showing constraints from CMB  $C_\ell^{TT,TE,EE}$  and lensing potential from Plk18, and continue by adding BAO first, then  $f\sigma_8$  growth measurements next, to finish with DES  $3 \times 2$ pt galaxy clustering and lensing probes. This order is motivated by what each probe is expected to add as additional constraints on our three beyond  $\Lambda$ CDM

<sup>1</sup><https://gitlab.com/zizgitlab/mgclass--ii>

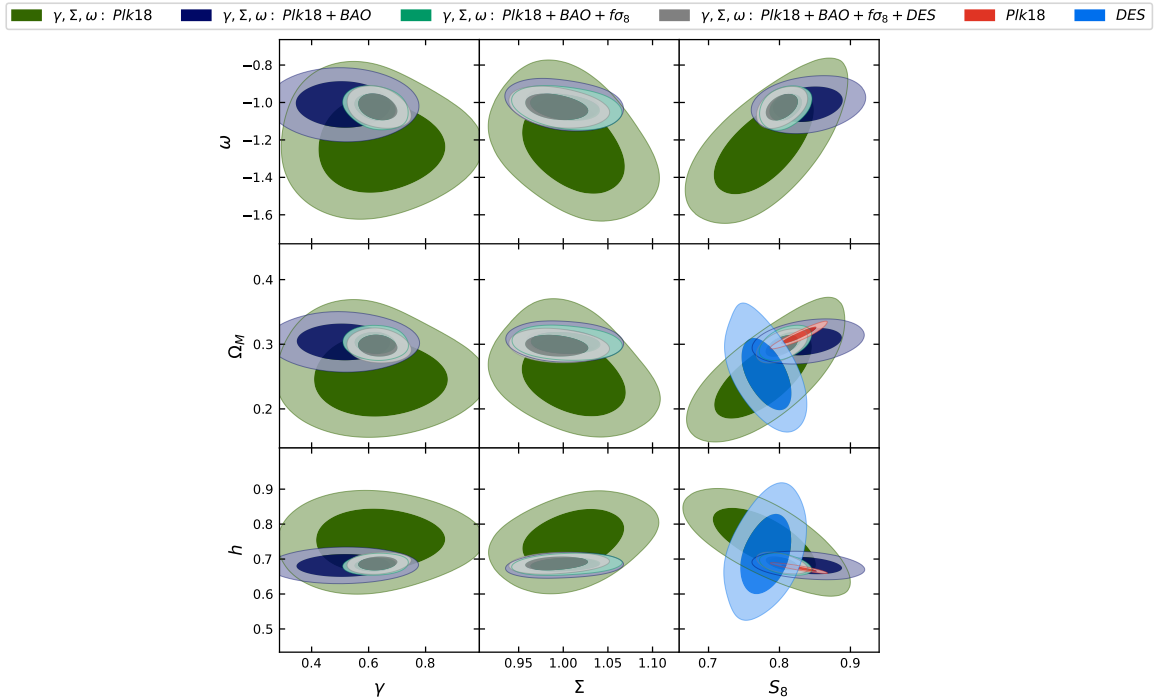


**Figure 1.** 68% and 95% confidence contours for  $\Omega_m$ ,  $h$ ,  $w$ ,  $S_8$ ,  $\gamma$  and  $\Sigma$  inferred from different combinations of: CMB  $C_\ell^{TT,TE,EE}$  and its lensing potential from Plk18, BAO observations,  $f\sigma_8$  measurements and 3x2pt photometric lensing and galaxy correlations and cross correlations from DES survey.

parameters. As so, CMB temperature and polarisation angular power spectrum and its extracted lensing quadrupole probe will start by putting constraints on some or all of our beyond  $\Lambda$ CDM parameters as seen in [32] and [23] as well as [16]. Next BAO is expected to additionally constrain notably  $w$  without much effect on the growth and lensing parameters, that are then respectively constrained by the addition of the redshift space distortions data and the lensing from DES data. The latter with the galaxy clustering data will especially constrain the growth and lensing MG parameters from the leverage gained from observations covering  $0 < z < 1.5$ , combined with higher redshifts from CMB lensing power spectrum that are mainly sensitive to large scale structure around  $z \sim 2$ . For the two models, the constant or dynamical  $\Sigma$  one, we also show  $\Lambda$ CDM constraints from Plk18 data and DES  $3 \times 2$ pt data separately to get better insights about how the constraints are changing with respect to the standard cosmological model. For the two models, either  $\Sigma$  constant or parameterised through  $\gamma_\ell$ , we observe that the Plk18 data allow much freedom for all of the triggering parameters (green lines) though still compatible with their equivalent  $\Lambda$ CDM values. We also notice that the constraints on  $S_8$  and  $h$  are loose so that the range covers the values subject of tensions between local and deep probes on these two parameter bounds (see [33–35] for more on this subject). In both parameterisations of  $\Sigma$ , we especially see  $w$  preferring far negative values as was the case in similar studies [28, 29] though it is showing stronger correlations with the other two beyond  $\Lambda$ CDM parameters for the model with dynamical  $\Sigma$ . As expected, adding BAO data strongly constrain  $w$  for both models (dark blue lines) as well as  $h$  and  $\Omega_m$  while having a small effect on the growth index  $\gamma$ . For the MG lensing parameter, we see also that the

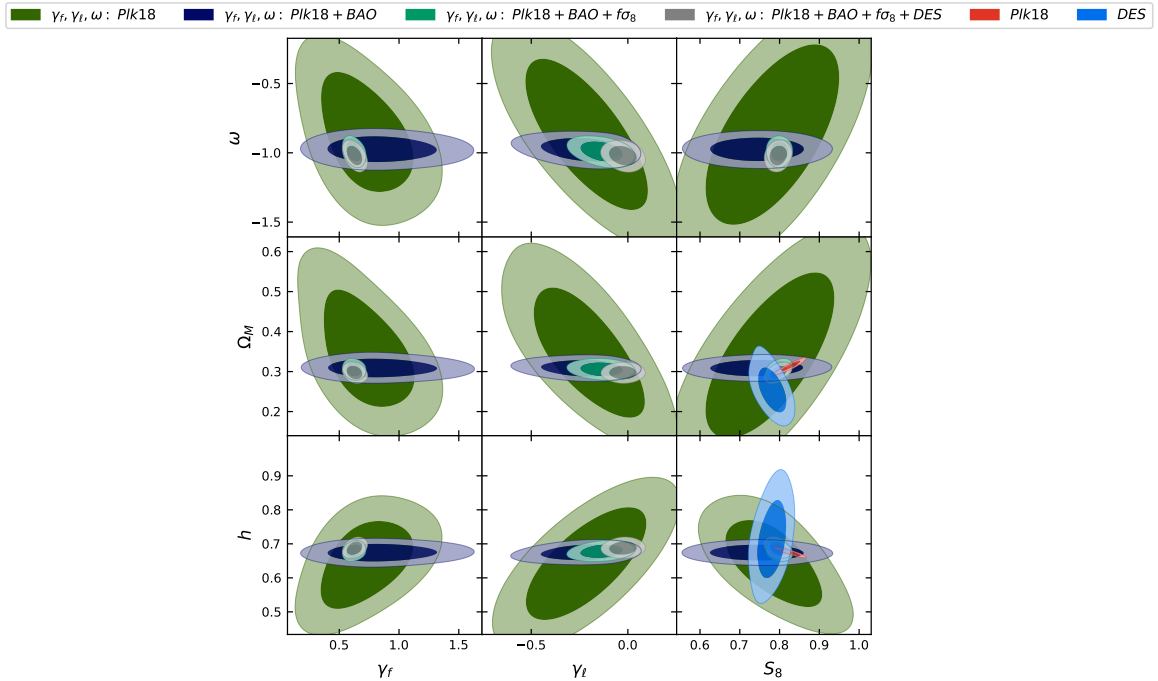


**Figure 2.** 68% and 95% confidence contours for  $\Omega_m$ ,  $h$ ,  $w$ ,  $S_8$ ,  $\gamma_f$  and  $\gamma_\ell$  from different combinations of: CMB  $C_\ell^{TT,TE,EE}$  and its lensing potential from Plk18, BAO observations,  $f\sigma_8$  measurements and 3x2pt photometric lensing and galaxy correlations and cross correlations from DES survey.

gain is small for  $\Sigma$  constant but is more substantial for  $\gamma_\ell$  due to the fact that we have broken the degeneracy on the latter when we strongly constrained other cosmological parameters especially  $\Omega_m$ , thus limiting the freedom for  $\Sigma = \Omega(z)^{\gamma_\ell}$  to vary. We also observe that all the parameters are still compatible with their equivalent  $\Lambda$ CDM values though the growth index  $\gamma$  is showing preference for values below 0.55 in the constant  $\Sigma$  case and the lensing index  $\gamma_\ell$  is preferring negative values for the dynamical  $\Sigma$  case. The reason for BAO not equally breaking degeneracy between matter density and the growth index as was the case for the lensing index is that  $\gamma$  has very little effect on the CMB perturbations where  $\Omega_m(z)$  value is at the level of unity at the recombination epoch. The situation substantially changes when we add growth data (light green lines), which mainly put strong constraints on the growth index  $\gamma$  for both models, while  $\Sigma$  constraints are almost unchanged in the first model and tighter for the second even if still preferring negative values. This comes from the fact that  $f\sigma_8$  measurements, by constraining  $\gamma$  are also doing the same for  $\Omega_m$  which also affects those on  $\gamma_\ell$ . We notice also that  $S_8$  is back in being in slight tension with its  $\Lambda$ CDM value, a fact later consolidated when we additionally add DES datasets. In the latter case, we see (gray lines) that DES data has not added much improvement on the growth index  $\gamma$  bounds in both cases although we see that the latter is now well constrained around 0.6 not far from its fiducial  $\Lambda$ CDM value. While for the MG lensing parameter  $\Sigma$ , we observe that the gain in the constant case is small with respect to what we already had from Plk18+BAO+RSD. However, the improvement is noticeable for the model with dynamical  $\Sigma$  that has been showing preferences for negative values but is now shifted to be well constrained around the null value corresponding to  $\Lambda$ CDM and GR. We show in table 1 and table 2 at the level of confidence at 68% the bounds obtained

	CMB	CMB + BAO	CMB + BAO + $f\sigma_8$	CMB + BAO + $f\sigma_8$ + DES
$\gamma$	$0.63\pm 0.11$	$0.518\pm 0.072$	$0.624\pm 0.046$	$0.633\pm 0.044$
$\omega$	$-1.23\pm 0.15$	$-1.009\pm 0.053$	$-1.025\pm 0.047$	$-1.025\pm 0.045$
$\Sigma$	$1.011\pm 0.032$	$0.998\pm 0.025$	$1.002\pm 0.024$	$0.992\pm 0.022$

**Table 1.** constraints at the 68% level of  $\omega$ ,  $\gamma$  and  $\Sigma$  inferred from different combinations of: CMB  $C_\ell^{TT,TE,EE}$  and its lensing potential from Plk18, BAO observations,  $f\sigma_8$  measurements and 3x2pt photometric lensing and galaxy correlations and cross correlations from DES survey.

by the different combinations in the two cases on the beyond  $\Lambda$ CDM parameters considered in this work. The values in all but especially the CMB+BAO case agree with the recent work of [36] limited to these probes while the most constraining case CMB+BAO+ $f\sigma_8$ +DES agrees well with another study using all these probes [37] albeit the fact that they followed instead the method of rescaling the power spectrum for a new value of  $\gamma$ , and that they did only considered one extra parameter  $\gamma$ . This is due to the fact that in the most constraining case  $\omega$  and  $\Sigma$  are close to their  $\Lambda$ CDM values.

These results could be further understood when looking at Fig. 3 and Fig. 4 where we show contours for the two models with further plots obtained from Plk18 without lensing while also emphasising on the evolution of the degeneracies and correlations between our beyond  $\Lambda$ CDM parameters throughout our different combinations. We also show the derived parameter  $\Sigma$  instead of  $\gamma_\ell$  to allow a better comparison between the two cases. We see first in Fig. 3 with the constant  $\Sigma$  case that there are no differences in the constraints on  $\gamma$  or  $\Sigma$  coming from the Plk18 lensing. The difference is seen however on those on  $\omega$  further favouring negative values without the lensing data since CMB lensing potential is affected by large scale structure at  $z \sim 2$  where  $\omega$  effects on formation of structure are noticeable at those redshifts. We also see a correlation and degeneracy between  $\Sigma$  and  $\gamma$  that is not broken by the BAO data until we add growth measurements and DES data while we observe a correlation between  $\Sigma$  and  $w$  which is not present between  $w$  and  $\gamma$  at the Plk18 only level since  $\Omega_m$  is close to one as mentioned before. That could explain why BAO was able of constraining also  $\Sigma$  so well since it does so for the correlated parameter  $\omega$ . While for the case where  $\Sigma$  is parameterised function of  $\gamma_\ell$  we observe in Fig. 4 the same behaviour as the first case with respect to  $\omega$  but a different one for the  $\Sigma - \gamma$  contours showing positive correlations at the level of Plk18 since now for both parameters the constrains are driven by  $\Omega_m$  with less constraints from CMB at the recombination epoch. Both parameters are also not correlated with  $\omega$  which explain why BAO have not the same effect as the  $\Sigma$  constant case. We also understand why  $f\sigma_8$  measurements were able of further constraining  $\Sigma$  even before further consolidation from DES since we observe that their addition breaks the degeneracy with  $\gamma$  allowing us to benefit from BAO and CMB constraint on the matter density parameter to reduce the contours on both  $\Sigma$  and  $\gamma$  parameters.

## 5 Conclusion

In this work we performed a Bayesian analysis to obtain simultaneous constraints on three parameters commonly used to test deviations from  $\Lambda$ CDM, namely the dark energy equation of state parameter  $\omega$ , the growth index  $\gamma$  and the Weyl potential parameter  $\Sigma$  and that in a consistent way within the same Boltzmann and cosmological solver used to compute the

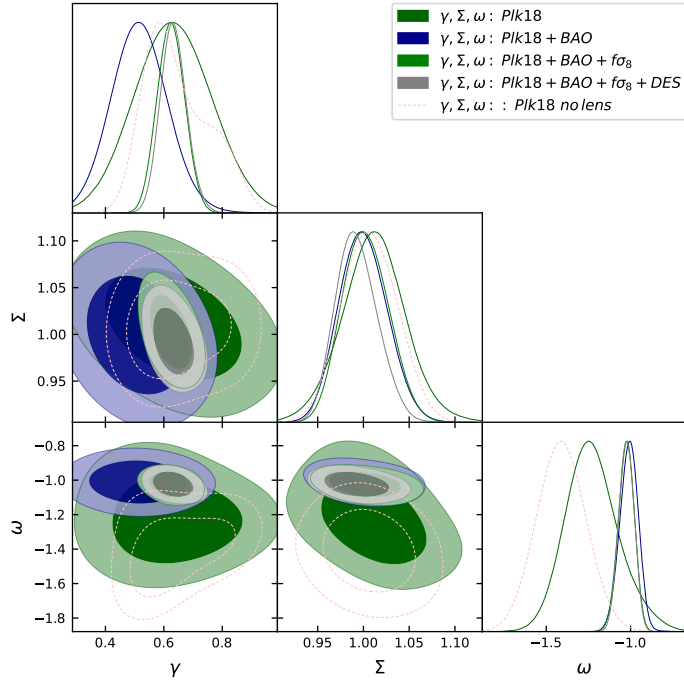


**Figure 3.** 68% and 95% confidence contours for  $\gamma$ ,  $\Sigma$  and  $\omega$ , inferred from different combinations of: CMB  $C_\ell^{TT,TE,EE}$  and its lensing potential from Plk18, BAO observations,  $f\sigma_8$  measurements and 3x2pt photometric lensing and galaxy correlations and cross correlations from DES survey; in comparison to the same combinations but using CMB  $C_\ell^{TT,TE,EE}$  from Plk18 alone.

	CMB	CMB, BAO	CMB, BAO, $f\sigma_8$	CMB, BAO, $f\sigma_8 + \text{DES}$
$\gamma_f$	$0.72 \pm 0.22$	$0.86 \pm 0.27$	$0.622 \pm 0.040$	$0.628 \pm 0.040$
$\omega$	$-0.87 \pm 0.24$	$-0.975 \pm 0.051$	$-0.991 \pm 0.046$	$-1.021 \pm 0.045$
$\gamma_\ell$	$-0.22 \pm 0.13$	$-0.24 \pm 0.13$	$-0.135 \pm 0.070$	$-0.025 \pm 0.045$

**Table 2.** constraints at the 68% level of  $\gamma_f$ ,  $\omega$  and  $\gamma_\ell$  inferred from different combinations of: CMB  $C_\ell^{TT,TE,EE}$  and its lensing potential from Plk18, BAO observations,  $f\sigma_8$  measurements and 3x2pt photometric lensing and galaxy correlations and cross correlations from DES survey.

different theoretical observables used within the new cosmologies. The analysis was conducted using different combinations of CMB  $TT, TE, EE$  and lensing  $C_{\ell_s}$ , BAO observations,  $f\sigma_8$  measurements and 3x2pt photo lensing and galaxy correlations and their cross correlations, and that considering two parameterisation for  $\Sigma$ , first as a constant and second following a similar approach usually performed for the growth index  $\gamma_f$ , by formulating it as function of the matter density at a certain redshift elevated to a lensing index  $\gamma_\ell$  introduced for the first time in this work. For the case of a constant  $\Sigma$ , we found that the CMB data still allows deviations from  $\Lambda\text{CDM}$  though still compatible with the latter, while adding BAO strongly constrains the  $\omega$  parameter and that from the impact of the latter on the background evolution, but also and to a lesser extent it constrains the lensing parameter  $\Sigma$  after breaking the degeneracies between the latter and the other cosmological parameters such as  $\Omega_m$  and  $h$ . Adding the growth  $f\sigma_8$  measurements and the clustering and lensing correlations of galaxies then strongly limits the bounds on  $\Sigma$  and those on the growth index despite a shift to values

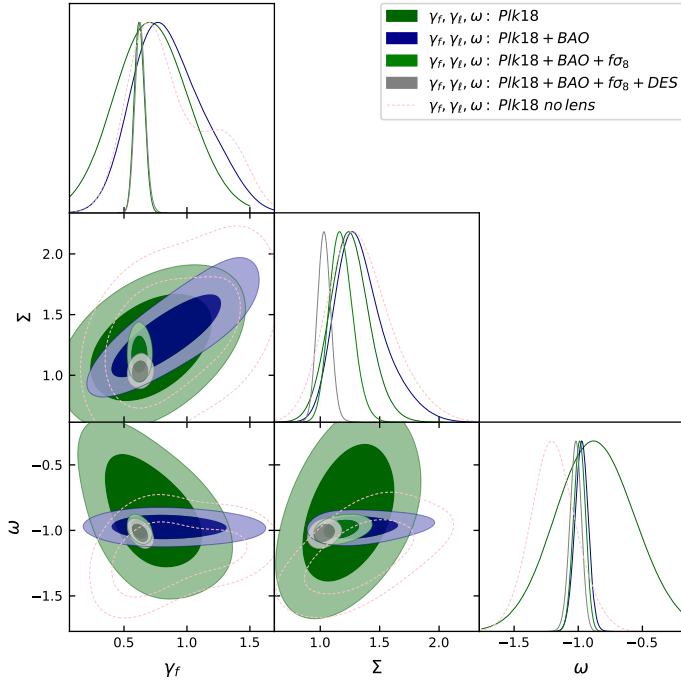


**Figure 4.** 68% and 95% confidence contours for  $\gamma_f$ ,  $\omega$  and  $\Sigma$  derived from  $\gamma_\ell$  following Equ. 2.8 inferred from different combinations of: CMB  $C_\ell^{TT,TE,EE}$  and its lensing potential from Plk18, BAO observations,  $f\sigma_8$  measurements and 3x2pt photometric lensing and galaxy correlations and cross correlations from DES survey; in comparison to the same combinations but using CMB  $C_\ell^{TT,TE,EE}$  from Plk18 alone.

still within  $2\sigma$  from its  $\Lambda$ CDM ones. For the case where we parameterise  $\Sigma$  as function of the matter density and a lensing index  $\gamma_\ell$ , we found strong degeneracies between the aforementioned parameters due to the common presence of matter density ingredient when constrained only by CMB data and the addition of BAO was only able of breaking those on  $\omega$  while a combination with the  $f\sigma_8$  data was needed to constrain the growth index  $\gamma_f$  to within  $2\sigma$  from its fiducial value. Still the lensing index  $\gamma_\ell$  was showing preference for negative values even though compatible with  $\Lambda$ CDM and that until the clustering and lensing correlations of galaxies were further added, bringing it back to having a maximum likelihood close to its equivalent  $\Lambda$ CDM value. We conclude that  $\Lambda$ CDM is still compatible with a combination of the large cosmological datasets used in this work despite the three phenomenological model extensions adopted and a mild tension for  $\gamma$  and that a similar parameterisation for the lensing and growth of structure function of the matter density, offers room for substantial deviation from general relativity, especially for the Weyl potential parameter, which was not strongly constrained until we combined all of the datasets used in this work.

## Acknowledgments

Z.S. acknowledges funding from DFG project 456622116 and support from the IRAP Toulouse and IN2P3 Lyon computing centres.

## References

- [1] Jerome Martin. Everything You Always Wanted To Know About The Cosmological Constant Problem (But Were Afraid To Ask). *Comptes Rendus Physique*, 13:566–665, 2012.
- [2] Timothy Clifton, Pedro G. Ferreira, Antonio Padilla, and Constantinos Skordis. Modified Gravity and Cosmology. *Phys. Rept.*, 513:1–189, 2012.
- [3] M. Chevallier and D. Polarski. Accelerating Universes with Scaling Dark Matter. *International Journal of Modern Physics D*, 10:213–223, 2001.
- [4] E. V. Linder. Exploring the Expansion History of the Universe. *Physical Review Letters*, 90(9):091301, March 2003.
- [5] James M. Bardeen. Gauge Invariant Cosmological Perturbations. *Phys. Rev. D*, 22:1882–1905, 1980.
- [6] Viatcheslav F. Mukhanov, H. A. Feldman, and Robert H. Brandenberger. Theory of cosmological perturbations. Part 1. Classical perturbations. Part 2. Quantum theory of perturbations. Part 3. Extensions. *Phys. Rept.*, 215:203–333, 1992.
- [7] Pengjie Zhang, Michele Liguori, Rachel Bean, and Scott Dodelson. Probing Gravity at Cosmological Scales by Measurements which Test the Relationship between Gravitational Lensing and Matter Overdensity. *Phys. Rev. Lett.*, 99:141302, 2007.
- [8] Karim A. Malik and David Wands. Cosmological perturbations. *Phys. Rept.*, 475:1–51, 2009.
- [9] Luca Amendola, Martin Kunz, and Domenico Sapone. Measuring the dark side (with weak lensing). *JCAP*, 04:013, 2008.
- [10] Levon Pogosian, Alessandra Silvestri, Kazuya Koyama, and Gong-Bo Zhao. How to optimally parametrize deviations from General Relativity in the evolution of cosmological perturbations? *Phys. Rev. D*, 81:104023, 2010.
- [11] Jolyon Bloomfield. A Simplified Approach to General Scalar-Tensor Theories. *JCAP*, 12:044, 2013.
- [12] Noemi Frusciante and Louis Perenon. Effective field theory of dark energy: A review. *Phys. Rept.*, 857:1–63, 2020.
- [13] E. V. Linder. Cosmic growth history and expansion history. *PRD*, 72(4):043529, August 2005.
- [14] Eva-Maria Mueller, Will Percival, Eric Linder, Shadab Alam, Gong-Bo Zhao, Ariel G. Sánchez, Florian Beutler, and Jon Brinkmann. The clustering of galaxies in the completed SDSS-III Baryon Oscillation Spectroscopic Survey: constraining modified gravity. *Mon. Not. Roy. Astron. Soc.*, 475(2):2122–2131, 2018.
- [15] Bin Hu, Michele Liguori, Nicola Bartolo, and Sabino Matarrese. Parametrized modified gravity constraints after Planck. *Phys. Rev. D*, 88(12):123514, 2013.
- [16] Ziad Sakr and Matteo Martinelli. Cosmological constraints on sub-horizon scales modified gravity theories with MGCLASS II. *JCAP*, 05(05):030, 2022.
- [17] D. Blas, J. Lesgourgues, and T. Tram. The Cosmic Linear Anisotropy Solving System (CLASS). Part II: Approximation schemes. *JCAP*, 7:034, July 2011.
- [18] Seyed Hamidreza Mirpoorian, Zhuangfei Wang, and Levon Pogosian. On validity of the quasi-static approximation in scalar-tensor theories. 2 2023.
- [19] Tessa Baker and Philip Bull. Observational signatures of modified gravity on ultra-large scales. *Astrophys. J.*, 811:116, 2015.
- [20] R. Calderon, D. Felbacq, R. Gannouji, D. Polarski, and A. A. Starobinsky. Global properties of the growth index of matter inhomogeneities in the universe. *Phys. Rev. D*, 100(8):083503, 2019.

- [21] Yuewei Wen, Nhat-Minh Nguyen, and Dragan Huterer. Sweeping Horndeski Canvas: New Growth-Rate Parameterization for Modified-Gravity Theories. 4 2023.
- [22] N. Aghanim et al. Planck 2018 results. V. CMB power spectra and likelihoods. *Astron. Astrophys.*, 641:A5, 2020.
- [23] N. Aghanim et al. Planck 2018 results. VI. Cosmological parameters. *Astron. Astrophys.*, 641:A6, 2020. [Erratum: *Astron. Astrophys.* 652, C4 (2021)].
- [24] Florian Beutler, Chris Blake, Matthew Colless, D. Heath Jones, Lister Staveley-Smith, Lachlan Campbell, Quentin Parker, Will Saunders, and Fred Watson. The 6dF Galaxy Survey: Baryon Acoustic Oscillations and the Local Hubble Constant. *Mon. Not. Roy. Astron. Soc.*, 416:3017–3032, 2011.
- [25] Ashley J. Ross, Lado Samushia, Cullan Howlett, Will J. Percival, Angela Burden, and Marc Manera. The clustering of the SDSS DR7 main Galaxy sample – I. A 4 per cent distance measure at  $z = 0.15$ . *Mon. Not. Roy. Astron. Soc.*, 449(1):835–847, 2015.
- [26] Shadab Alam et al. The clustering of galaxies in the completed SDSS-III Baryon Oscillation Spectroscopic Survey: cosmological analysis of the DR12 galaxy sample. *Mon. Not. Roy. Astron. Soc.*, 470(3):2617–2652, 2017.
- [27] Bryan Sagredo, Savvas Nesseris, and Domenico Sapone. Internal Robustness of Growth Rate data. *Phys. Rev. D*, 98(8):3, 2018.
- [28] T. M. C. Abbott et al. Dark Energy Survey year 1 results: Cosmological constraints from galaxy clustering and weak lensing. *Phys. Rev. D*, 98(4):043526, 2018.
- [29] T. M. C. Abbott et al. Dark Energy Survey Year 3 results: Cosmological constraints from galaxy clustering and weak lensing. *Phys. Rev. D*, 105(2):023520, 2022.
- [30] B. Audren, J. Lesgourgues, K. Benabed, and S. Prunet. Conservative constraints on early cosmology with MONTE PYTHON. *JCAP*, 2:001, February 2013.
- [31] Rubén Arjona, Juan García-Bellido, and Savvas Nesseris. Cosmological constraints on nonadiabatic dark energy perturbations. *Phys. Rev. D*, 102(10):103526, 2020.
- [32] P. A. R. Ade et al. Planck 2015 results. XIV. Dark energy and modified gravity. *Astron. Astrophys.*, 594:A14, 2016.
- [33] Leandros Perivolaropoulos and Foteini Skara. Challenges for  $\Lambda$ CDM: An update. *New Astron. Rev.*, 95:101659, 2022.
- [34] Eleonora Di Valentino, Olga Mena, Supriya Pan, Luca Visinelli, Weiqiang Yang, Alessandro Melchiorri, David F. Mota, Adam G. Riess, and Joseph Silk. In the realm of the Hubble tension—a review of solutions. *Class. Quant. Grav.*, 38(15):153001, 2021.
- [35] Ziad Sakr, Stephane Ilic, and Alain Blanchard. Cluster counts - III.  $\Lambda$ CDM extensions and the cluster tension. *Astron. Astrophys.*, 666:A34, 2022.
- [36] Enrico Specogna, Eleonora Di Valentino, Jackson Levi Said, and Nhat-Minh Nguyen. Exploring the Growth Index  $\gamma_L$ : Insights from Different CMB Dataset Combinations and Approaches. 5 2023.
- [37] Nhat-Minh Nguyen, Dragan Huterer, and Yuewei Wen. Evidence for suppression of structure growth in the concordance cosmological model. 2 2023.